Macromolecules

ARTICLE

pubs.acs.org/Macromolecules

Quaterthiophene–Benzobisazole Copolymers for Photovoltaic Cells: Effect of Heteroatom Placement and Substitution on the Optical and Electronic Properties

Achala Bhuwalka,[†] Jared F. Mike,[†] Meng He,[‡,§] Jeremy J. Intemann,[†] Toby Nelson,[∥] Monique D. Ewan,[†] Robert A. Roggers,[†] Zhiqun Lin,[‡,⊥] and Malika Jeffries-EL*[,†]

[†]Department of Chemistry, Iowa State University, Ames Iowa 50011, United States

[‡]Department of Materials Science and Engineering, Iowa State University, Ames, Iowa 50011, United States

[§]The Key Laboratory of Molecular Engineering of Polymers, Ministry of Education, Department of Macromolecular Science, Fudan University, Shanghai 200433, China

[∥]Department of Chemistry, Carnegie Mellon University, Pittsburgh, Pennsylvania 15213, United States

[⊥]School of Materials Science and Engineering, Georgia Institute of Technology, Atlanta, Georgia 30332, United States

Supporting Information

ABSTRACT: Three new donor–acceptor conjugated polymers were synthesized by combining electron-donating 3-octylthiophenes with various electron-accepting benzobisazoles. The influence of the structural differences of the three benzobisazoles on the electrochemical, optical, and photovoltaic properties of the polymers composed from them was investigated. According to our results, changing the arrangement of the oxygen atoms of the benzobisoxzoles from the *cis* to *trans* orientation slightly stabilized both the HOMO and LUMO levels, whereas replacing the oxygen atoms in *trans*-BBO with sulfur atoms only stabilized the HOMO level. Bulk heterojunction photovoltaic devices were fabricated by using the copolymers as electron donors and $PC_{71}BM$ ([6,6]-phenyl C_{71}-butyric acid methyl ester). It was found that open-circuit voltages (V_{oc}s) as high as 0.86 V, and power conversion efficiencies (PCEs) up to 1.14%, were obtained under simulated AM 1.5 solar irradiation of 100 mW/cm^2. Field-effect transistors based on these polymers exhibited hole mobilities as high as of 4.9×10^{-3} cm^2/(V s) with the *trans*-BBO polymer giving the best performance in both devices.

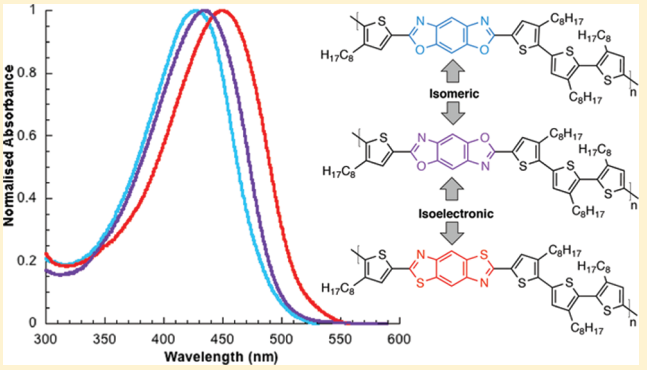

INTRODUCTION

In recent years, conjugated polymers have generated a large amount of interest as potential replacements for inorganic semiconductors in applications such as organic light-emitting diodes (OLEDs),[1−3] photovoltaic cells[4−6] (PVCs), and field-effect transistors (FETs).[7] It is generally understood that organic semiconductors have several major advantages over their inorganic counterparts, including the ability to fabricate lightweight flexible devices, the opportunity to make large area devices using low-cost solution-based techniques, and the variety of optical and electronic properties that can be attained through chemical synthesis.[8−12] Currently, a popular strategy for tailoring of the properties of conjugated polymers is through the synthesis of materials composed of alternating electron-donating and electron-accepting groups.[13−15] This approach has produced a number of useful materials resulting in charge carrier mobilities exceeding 0.1 cm^2 V^{-1} s^{-1} in FETs and record performances of greater than 8% in PVCs.[15−21] Although conjugated polymer PVCs are rapidly approaching the minimum 10% efficiency required for commercial viability,[5] the development of new materials with improved properties and easy synthetic routes remains a challenge.[16−20]

On the basis of the aforementioned considerations, we became interested in the development of new materials based on the benzobisoxazole and benzobisthiazole moieties. Collectively known as benzobisazoles,[22] these planar, electron-deficient heterocycles were initially used for the synthesis of rigid-rod polymers with excellent tensile strength and thermal stability.[23−25] As a result of their origins as high-performance materials, the requisite starting materials for the synthesis of benzobisazoles are readily prepared on a large scale and in good yield.[23,24,26,27] Although the incorporation of benzobisazoles into conjugated materials is known to enhance the electron transport,[28,29] photoluminescence,[30−33] and third-order nonlinear

Received: September 20, 2011
Revised: November 8, 2011
Published: November 28, 2011

ACS Publications © 2011 American Chemical Society

Scheme 1. Synthesis of Thiophene−Benzobisazole Copolymers

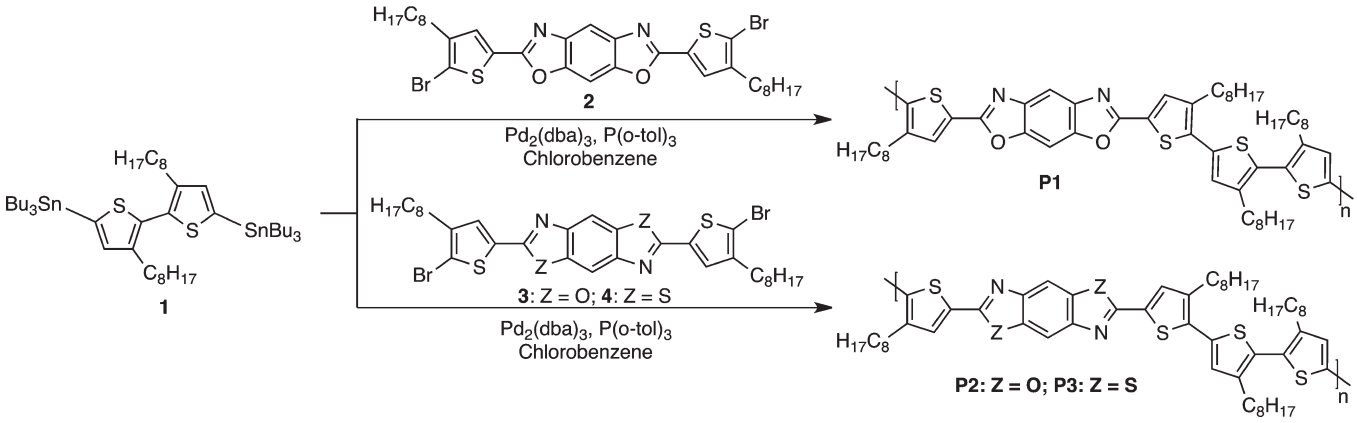

optical properties,[34−37] until recently, their use has been hindered by poor solubility and the harsh conditions used for their synthesis.[38−50] This is particularly problematic for the synthesis of materials based on benzo[1,2-*d*;4,5-*d*′]bisoxazole (*trans*-BBO); as the starting material for its synthesis, 2,5-diaminohydroquinone readily decomposes.[39]

Previous research on the optical and electronic properties of benzo[1,2-*d*;5,4-*d*′]bisoxazole (*cis*-BBO) and benzo[1,2-*d*;4,5-*d*′]bisthiazole (*trans*-BBZT) indicates that replacing oxygen with the less electronegative sulfur atom increases the delocalization within the π-orbitals.[10−12,15] Additionally, the empty d-orbitals of the sulfur atom can contribute to the molecular π-orbitals, decreasing the energy of the $\pi-\pi^*$ transition.[28−37,49,51−54] However, since materials containing the analogous *trans*-BBO had not been synthesized, the influence of the heteroatom position on the optical and electronic properties of materials containing benzobisoxazoles has not been investigated. Varying the arrangement of the oxygen atoms around the central benzene ring impacts the planarity of the benzobisoxazoles, their symmetry, and also their dipole moments.[44,55] In order to investigate the influence of these modifications on the properties of the resulting polymers, we have synthesized three new alternating copolymers containing *trans*-BBO, *cis*-BBO, and the analogous sulfur compound (*trans*-BBZT) as the accepting group and an electron-donating 3,3″,3‴,4′-tetraoctyl-2,2′:5′,2″:5″,2‴-quaterthiophene unit. The thiophene-based comonomer was used to improve the solubility and hole mobility of the resulting copolymers.

RESULTS AND DISCUSSION

Synthesis. The chemical structures and synthetic routes toward the three polymers are outlined in Scheme 1. We elected to first synthesize monomers where the benzobisazole moiety is positioned between two thiophene rings as this building block allows for polymerization to be performed using transition-metal-catalyzed cross-coupling reactions, instead of condensation polymerization. The requisite monomers 2,6-bis(4-octylthiophen-2-yl)benzo[1,2-*d*;5,4-*d*′]bisoxazole (**2**), 2,6-bis(4-octylthiophen-2-yl)benzo[1,2-*d*;4,5-*d*′]bisoxazole (**3**), and 2,6-bis(4-octylthiophen-2-yl)benzo[1,2-*d*;4,5-*d*′]bisthiazole (**4**) were synthesized in high yields (78−84%) according to the literature procedure.[56] Unfortunately, we are unable to synthesize the fourth derivative, 2,6-bis(4-octylthiophen-2-yl)-benzo[1,2-*d*;5,4-*d*′]bisthiazole, which contains the *cis*-BBZT moiety due to the lack of protocols for the synthesis of the required starting material 4,6-diaminobenzene 1,3-dithiol. There are no reports for the synthesis of this compound in the modern literature, and all attempts to develop a new approach were unsuccessful.

Table 1. Physical Properties of Thiophene−Benzobisazole Copolymers

polymer	M_n[a]	% yield	PDI	T_d (°C)[b]	T_g (°C)[c]
P1	9900	60	1.37	374	84.2
P2	8200	65	1.39	401	84.6
P3	5000	55	1.69	324	80.8

[a] Determined by GPC in THF using polystyrene standards. [b] 5% weight loss temperature by TGA in air. [c] Data from second scan reported, heating rate 15 °C/min under N_2.

The Stille cross-coupling polymerization of monomers **2**, **3**, or **4** with (3,3′-dioctyl-2,2′-bithiophene-5,5′-diyl)bis(tributylstannane) (**1**) afforded the polymers **P1**, **P2**, and **P3**, respectively. All polymers were obtained in 55−65% yields after purification by Soxhlet extraction with methanol to remove residual catalyst followed by hexanes to remove the lower molecular weight material. The polymer was then isolated using THF as the extraction solvent. The solvent was evaporated, and the polymer so obtained was used for further analysis. All polymers are soluble in standard organic solvents, such as THF, *m*-cresol, and chloroform at room temperature, facilitating characterization using ^{1}H NMR spectroscopy and gel permeation chromatography (GPC). The ^{1}H NMR spectra for all polymers were in agreement with the proposed polymer structures (Figures S10, S11, and S12, Supporting Information). The number-averaged degree of polymerization (DP_n) ranged from 8 to 14, and despite the modest molecular weights, all of the polymers showed excellent film-forming ability. Thermogravimetric analysis (TGA) revealed that all polymers were thermally stable with 5% weight loss onsets occurring above 340 °C under air (Figure S2). All polymers exhibited weak glass transitions as measured by differential scanning calorimetry (DSC) (Figure S3). The results are summarized in Table 1.

Optical and Electrochemical Properties. The normalized absorbance spectra of the polymer solutions in THF and in the solid state are shown in Figures 1 and 2, respectively, and the data are summarized in Table 2. In solution, the UV spectra for all

three polymers exhibit a single, featureless absorbance band. As a result of changing the arrangement of the oxygen atoms, the absorption maximum for **P2** was red-shifted 7 nm relative to the absorbance maximum for **P1**. Substituting sulfur for oxygen results in a 16 nm red shift (relative to **P2**) in the absorption maximum of **P3** (and 23 nm relative to **P1**).

As thin films, the absorbance spectra for all polymers are significantly broader, resulting in bathochromic shifts in the absorption maximum, indicating increased backbone planarization and π-stacking in the solid state.[57] Interestingly, the spectra of **P1** and **P2** are significantly broader than that of **P3**, and they also exhibit a small shoulder at higher wavelengths, which is indication of strong interchain interactions in the solid state.[47] The presence of long-range order in the solid state is also supported by X-ray analysis, which shows that thin films of all polymers show periodicity (Figure S14). The diminished impact of the solid-state interactions within films of **P3** may be a result of its lower molecular weight. Jenekhe also observed differences in the solid-state absorption spectra for the related copolymer composed of 2,6-bis(5-bromo-3-octylthiophen-2-yl)benzo[1,2-*d*;4,5-*d*′]bisthiazole and (4,4′-dioctyl-2,2′-bithiophene-5,5′-diyl)-bis(trimethylstannane) (PBTOT) when the molecular weight of the polymer was increased.[47] The λ_{max}^{abs} of the benzobisthiazole polymer **P3** is also blue-shifted relative to the λ_{max}^{abs} reported previously for the related polymer PBTOT (λ_{max}^{abs} 540−551 nm).[47] This is most likely due to the different substitution pattern of the 3-alkylthiophene comonomers as PBTOT contains a tail-to-tail orientation of alkylthiophenes within the quaterthiophene unit, whereas **P3** contains a head-to-head defect. Such defects are known the decrease planarity, disrupting conjugation and resulting in an increase in the optical band gaps within poly(3-alkylthiophene)s.[58−60]

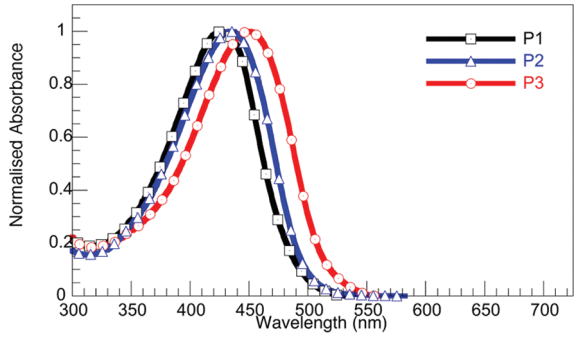

Figure 1. UV−vis absorption spectra of thiophene−benzobisazole copolymers in THF.

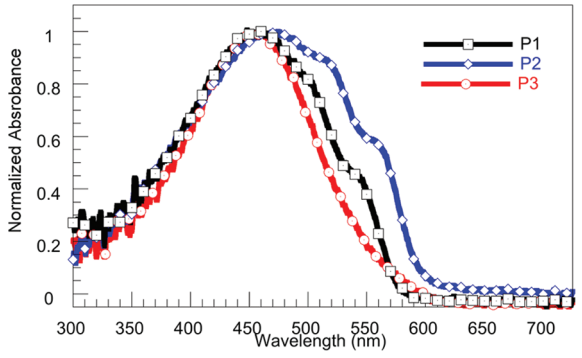

Figure 2. UV−vis absorption spectra of the thiophene−benzobisazole copolymers in the solid state. Thin films were spun from solutions of the polymers in *o*-DCB (2 mg/mL).

The optical band gaps of the benzobisazole polymers ranged from 2.1 to 2.2 eV and are larger than the 1.9 eV reported for the homopolymer poly(3-octylthiophene) (P3OT).[58] The fact that the donor−acceptor copolymer has a larger optical band gap than the homopolymer suggests that there is no significant intramolecular charge transfer within the polymer backbone.[61] The bandgaps of the benzobisoxazole polymers **P1** and **P2** are similar to the reported values for the related poly(thiophenevinylene-*co*-benzobisoxazole)s (2.0−2.2 eV), which were demonstrated to have limited distribution of electron density along the polymer backbone using density functional theory at the B3LYP/6-31G* level.[44] The poly(thiophenevinylene-*co*-benzobisoxazole)s also exhibited broader spectra with λ_{max}^{abs} that are significantly red-shifted relative to **P1** and **P2** (solution λ_{max}^{abs} 470−480 nm; film λ_{max}^{abs} 527−556 nm),[44] which is not surprising as the vinylene linkage minimizes steric interactions between consecutive aromatic rings, planarizing the polymer backbone and extending the π-conjugation, which can produce a more broadly absorbing material.[62,63] The electronic properties of the polymers were investigated by ultraviolet photoelectron spectroscopy (UPS) and differential pulse voltammetry (DPV). The onsets were internally referenced to Fc/Fc^+. In comparison to CV, DPV is more sensitive to oxidation and reduction potential onsets.[63,64] The electrochemical results are shown in Figures S3 and summarized in Table 2. All of the polymers exhibit measurable and reproducible oxidation and reduction processes. The HOMO levels were also determined using UPS, which accurately determines the HOMO level by bombarding an organic thin film with ultraviolet photons and measuring the kinetic energies of the ejected valence electrons.[65] In all cases, the values obtained for the HOMO levels using UPS match well with the values obtained using DPV. According to the UPS data, **P1**, **P2**, and **P3**

Table 2. Electronic and Optical Properties of Quaterthiophene−Benzobisazole Copolymers

	solution	film							
polymer	λ_{abs} (nm)	λ_{abs} (nm)	λ_{onset} (nm)	E_g^{opt} (eV)[a]	E_g^{ec} (eV)	E_{onset}^{ox}	E_{onset}^{red}	LUMO (eV)	HOMO (eV)
P1	427	460	580	2.2	2.4	0.54	−1.88	−2.9[b]/−2.9[c]	−5.1[d]/−5.3[e]
P2	434	475	597	2.1	2.3	0.57	−1.94	−3.1[b]/−2.9[c]	−5.2[d]/−5.4[e]
P3	450	462	560	2.2	2.3	0.62	−1.97	−3.1[b]/−2.8[c]	−5.3[d]/−5.4[e]

[a] Estimated from the optical absorption edge. [b] LUMO = HOMO(obtained from UPS) + E_g^{opt} (eV). [c] LUMO = −4.8 − (E_{onset}^{red}) (eV). [d] Obtained using ultraviolet photoelectron spectroscopy. [e] HOMO = −4.8 − (E_{onset}^{ox}) (eV). Electrochemical properties were measured using a three-electrode cell (electrolyte: 0.1 mol/L $TBAPF_6$ in acetonitrile) with an Ag/Ag^+ reference electrode, a platinum auxiliary electrode, and a platinum button electrode as the working electrode. Reported values are referenced to Fc/Fc^+. Polymer films were drop cast from an *o*-DCB solution of the polymers on to the working electrode. All differential pulse voltammetry experiments were recorded at a scan rate of 50 mV/s.

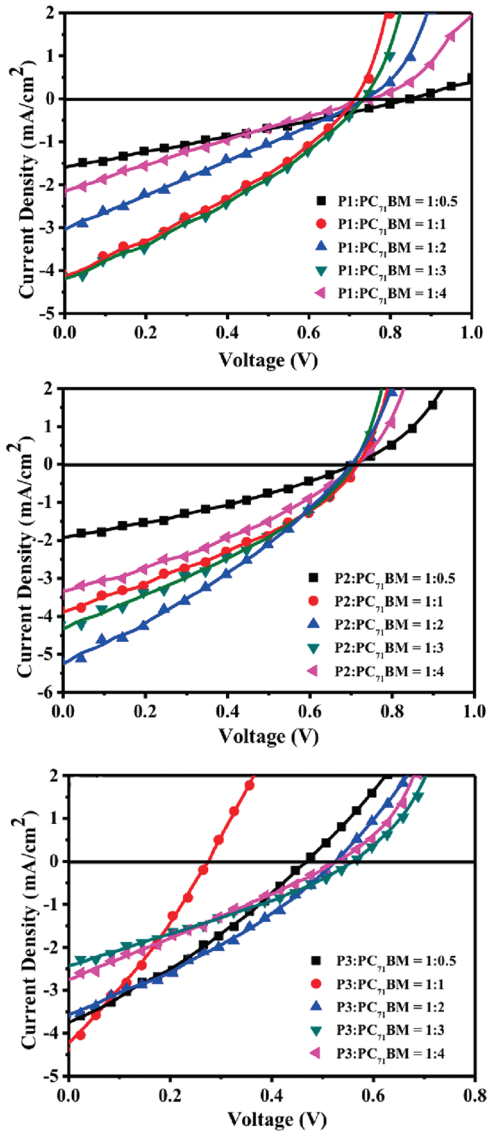

Figure 3. $J-V$ curves of bulk heterojunction solar cells fabricated from (a) **P3**/$PC_{71}BM$, (b) **P1**/$PC_{71}BM$, and (c) **P2**/$PC_{71}BM$ solar cells under AM 1.5 G illumination at 100 mW/cm^2. All the polymers and $PC_{71}BM$ were blended at different weight ratios (i.e., 1:0.5, 1:1, 1:2, 1:3, and 1:4).

exhibit HOMO levels of −5.1, −5.2, and −5.3 eV, respectively. These values are all lower than the reported HOMO of regioregular poly(3-hexylthiophene) (rr-P3HT) under the same conditions (−4.89 eV),[66] which means that these polymers are more stable against oxidation than rr-P3HT. Based on the UPS data, changing the position of the oxygen atoms from the *cis*-configuration to the *trans*-configuration stabilizes both the HOMO and LUMO levels, although the LUMO is influenced to a greater extent and thus **P2** has a smaller band gap than **P1**. The higher LUMO level of *cis*-BBO can be attributed to its inability to form a stable quinoidal state. Substituting sulfur atoms for the oxygen atoms in benzobisazoles stabilizes the HOMO but has no effect on the LUMO level, and thus **P3** has a larger band gap than **P2**. Since both *trans*-BBO and *trans*-BBZT can form stable quinoidal forms, the LUMO is unaffected by heteroatom substitution. However, since the sulfur atom is less electronegative than oxygen, *trans*-BBZT is more aromatic than *trans*-BBO. Thus, there is a greater delocalization of the electrons, resulting in a deeper HOMO. Overall the *trans*-BBO-based **P2** had the smallest bandgap of all of the polymers, whereas the *trans*-BBZT-based **P3** has the deepest HOMO level. The HOMO of the benzobisthiazole polymer **P3** is slightly lower than that reported previously for the related PBTOT (HOMO = −5.2 eV); however, **P3** has a slightly higher LUMO level (−3.1 eV) and thus a wider band gap.[47] These variances can be attributed to the different arrangement of the alkyl chains on the thiophene comonomers used in **P1**−**P3** and the error associated with cyclic voltammetry measurements.[58,67]

Table 3. OFET Characteristics of Benzobisazole−Quarterthiophene Copolymers

polymer	on/off ratio	μ_h^{max} (cm^2/(V s))	V_T (V)
P1	10^4	4.8×10^{-5}	−48
P2	10^2	8.9×10^{-5}	−30
P3	10^4	1.0×10^{-4}	−30

Field-Effect Transistors. The FET characteristics of the benzobisazole−quaterthiophene copolymers were studied using a bottom-gate, top-contact thin film transistor configuration. Several different channel lengths were measured for each polymer, and the best results are summarized in Table S2. Before polymer deposition, the SiO_2 surface was treated with octyltrichlorosilane (OTS), which is a surface treatment that can improve the molecular ordering and enhance FET performance.[68] The details of the device fabrication are described in the Experimental Methods. Overall, the FETs based on **P2** gave the best performance with a maximum observed hole mobility, $\mu_h = 4.8 \times 10^{-3}$ cm^2/(V s), and an average hole mobility, $\mu_h = 3.6 \times 10^{-3}$ cm^2/(V s). **P3** exhibited the poorest performance, which is not surprising as FET performance can be correlated to the nanostructure of the polymer.[69] This has been shown to be somewhat dependent on the molecular weight of the polymer.

Photovoltaic Properties. Photovoltaic devices with a configuration of ITO/PEDOT:PSS/polymer:$PC_{71}BM$/Ca/Al were fabricated at different weight ratios of polymer to $PC_{71}BM$ in order to identify the best donor−acceptor mixing ratios for these newly designed donor−acceptor copolymers. The area of the photovoltaic devices was 0.10 ± 0.01 cm^2. The current density−voltage ($J-V$) curves of **P1**/$PC_{71}BM$, **P2**/$PC_{71}BM$, and **P3**/$PC_{71}BM$ photovoltaic devices under AM 1.5 G illumination (100 mW/cm^2) are shown in Figure 3. The photovoltaic performances are summarized in Table 3. For devices based on **P2**/$PC_{71}BM$ and **P3**/$PC_{71}BM$, the highest power conversion efficiencies (PCE) were obtained using polymer/$PC_{71}BM$ weight ratios of 1:2, with PCEs of 0.61% and 1.14%, respectively. For devices based on **P1**/$PC_{71}BM$, the best performance was obtained using polymer/$PC_{71}BM$ weight ratios of 1:3, with a PCE of 0.98%. These results indicate that the donor/acceptor networks formed within blended films of 1:2 or 1:3 wt/wt ratio of these thiophene−benzobisazole copolymers transported holes more efficiently than in 1:1 P3HT/PCBM blends.[70,71] Interestingly, the benzobisoxazole polymers **P1** and **P2** both exhibited higher open-circuit voltage, $V_{oc} > 0.70$ V, than both **P3** and rr-P3HT. In fact, although **P3** had the lowest-lying HOMO level of all of the polymers, it had the worst performance of all of the benzobisazole polymers. Overall, the highest PCE of 1.14% was

Table 4. Summary of Photovoltaic Performances of P1/$PC_{71}BM$, P2/$PC_{71}BM$, and P3/$PC_{71}BM$ Solar Cells with Different Blending Ratios under AM 1.5 G Illumination at 100 mW/cm^2

polymer	$PC_{71}BM$ ratio (w/w)	V_{oc} (V)	J_{sc} (mA cm^{-2})	FF (%)	PCE (%)
P1	1:0.5	0.86	1.61	26.38	0.36
	1:1	0.73	4.10	31.49	0.94
	1:2	0.75	2.94	26.71	0.59
	1:3	0.74	4.22	31.48	0.98
	1:4	0.76	2.09	24.49	0.39
P2	1:0.5	0.72	1.90	31.95	0.44
	1:1	0.73	3.92	32.86	0.94
	1:2	0.73	5.13	30.59	1.14
	1:3	0.72	4.20	33.56	1.01
	1:4	0.72	3.43	31.89	0.79
P3	1:0.5	0.48	3.66	30.75	0.54
	1:1	0.28	4.30	29.25	0.35
	1:2	0.53	3.52	32.62	0.61
	1:3	0.57	2.39	29.50	0.40
	1:4	0.54	2.65	28.03	0.40

obtained in **P2**/$PC_{71}BM$ based device with V_{oc} of 0.73 V, J_{sc} of 5.13 mA/cm^2, and fill factor (FF) of 30.6%. The improved performance of the *trans*-BBO-based polymers can be attributed to its higher hole mobility, smaller band gap, and broader and red-shifted absorption spectra relative to the other benzobisazoles.

The low-lying HOMO level of the thiophene−benzobisazole copolymers was expected to improve performance by increasing the V_{oc}. Unfortunately, the overall performance was limited by the relatively wide band gaps of the polymers. The relatively low FF for the devices (<60%) indicates that poor bulk-heterojunction nanostructures formed in the blends. Since the morphology of the polymer:$PC_{71}BM$ blend greatly impacts the overall performance of bulk heterojunction solar cells, we examined the morphology of blends of the best performing polymer, **P2**, and $PC_{71}BM$ using atomic force microscopy (AFM). The height and phase images of the blends **P2** and various weight ratios of $PC_{71}BM$ are shown in Figure 4. Although there are slight variations in the PVC performance of the different blends, they all formed fairly smooth films with small root-mean-square (rms) roughness of (0.37, 0.43, 0.30, and 0.40 nm), for the 1:1, 1:2, 1:3, and 1:4 **P2**:$PC_{71}BM$ ratios, respectively. The 3D AFM images also indicate that the polymers form slightly rounded grains, resulting in an slightly irregular film surface. However, since AFM only indicates the properties of surface morphology of the active layers, the degree of vertical phase segregation of the two components in these samples is unknown.[62] In order to improve performance, we must first improve the film morphology of these new polymer blended with fullerenes. Future studies will investigate the influence of side-chain modifications and solvent additives, both of which have been demonstrated to be promising in optimizing the film morphology in such donor−acceptor copolymers and could improve J_{sc} and FF in **P1**- and **P2**-based devices.[72] It is worth noting that thermal annealing treatments under different temperatures (i.e., 100, 120, 140, and 160 °C) were carried out to improve the film morphology of the blend films. However, the performances of the PVCs decreased after thermal annealing as summarized in Table S1 of the Supporting Information.

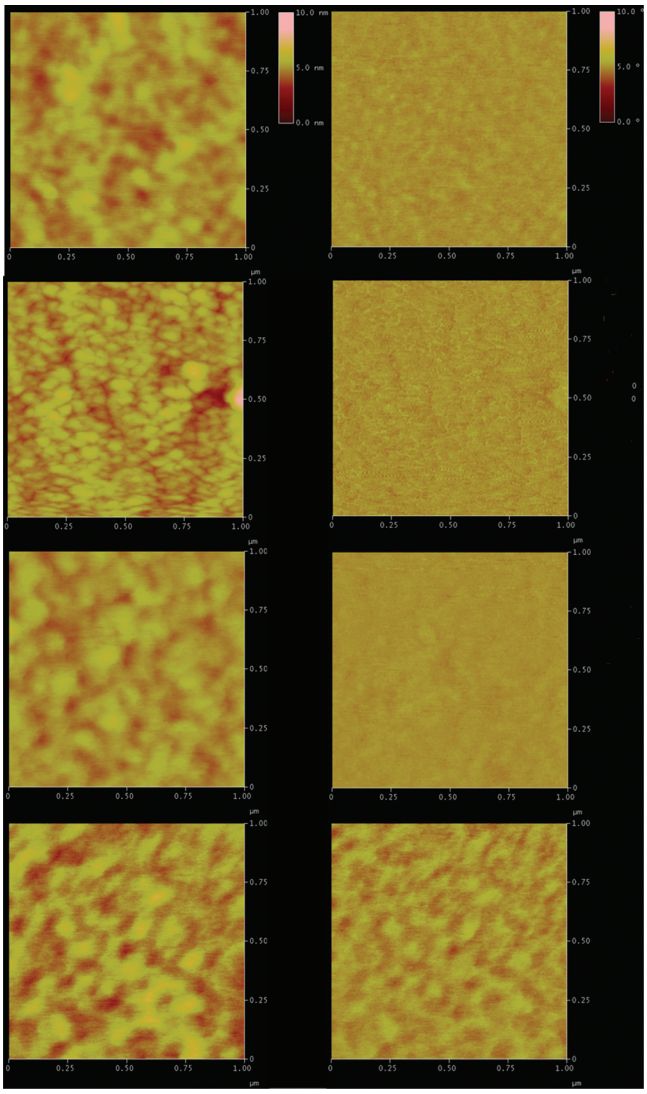

Figure 4. AFM height (left) and phase (right column) images of devices with various **P2**:$PC_{71}BM$ blends. From top to bottom: 1:1, 1:2, 1:3, and 1:4 **P2**:$PC_{71}BM$ ratios.

CONCLUSIONS

In summary, we have reported the synthesis of three related benzobisazole-containing polymers. The benzobisazole monomers were prepared in high yields and can be readily polymerized with bithiophene monomers via the Stille cross-coupling reaction. The octyl side chains on the thiophene rings led to good solubility, while maintaining good thermal stability. While the polymers have slightly different HOMO and LUMO levels, polymers based on *trans*-BBO exhibited broader and red-shifted absorption spectra relative to the other benzobisazoles in the solid state. The *trans*-BBO polymer **P2** also had the highest hole mobility of all three polymers. As a result of the ease of synthesis and deep HOMO level, *trans*-benzobisoxazoles have great potential for use in bulk heterojunction PVCs. We are currently synthesizing new derivatives of this polymer in order to improve its performance in photovoltaic cells and field-effect transistors.

EXPERIMENTAL METHODS

Materials and General Experimental Details. Tetrahydrofuran was dried using an Innovative Technologies solvent purification system. 2,6-Bis(4-octylthiophen-2-yl)benzo[1,2-*d*;5,4-*d*′]bisoxazole (**2**), 2,6-bis(4-octylthiophen-2-yl)benzo[1,2-*d*;4,5-*d*′]bisoxazole (**3**), 2,6-bis-(4-octylthiophen-2-yl)benzo[1,2-*d*;4,5-*d*′]bisthiazole (**4**), and (3,3′-dioctyl-2,2′-bithiophene-5,5′-diyl)bis(tributylstannane) (**1**) were synthesized according to literature procedures. All other compounds were purchased from commercial sources and used without further purification.

General Polymerization Procedure. A mixture of **1** and the respective benzobisazole, 2 mol % tris(dibenzylideneacetone)dipalladium(0), and 8 mol % tris-*o*-tolyphosphine in 12 mL of chlorobenzene was charged in a round-bottom flask equipped with a reflux condenser and an argon inlet. The mixture was allowed to reflux for 66 h before it was quenched by pouring into 100 mL of methanol containing 2% HCl. The precipitated polymer was filtered into a cellulose extraction thimble and then washed in a Soxhlet extractor with methanol, hexane, and THF. The polymer was recovered from the THF fractions after evaporation of the solvent.

Poly(2,6-bis(4-octyl-5-(3,3′-dioctylbithiophen-2-yl)thiophen-2-yl)benzo[1,2-*d*;5,4-*d*′]bisoxazole) (P1). Polymer obtained as a bright red solid (0.28 g, 60% yield). GPC: M_n = 9900, M_w = 13 600, PDI = 1.37.

Poly(2,6-bis(4-octyl-5-(3,3′-dioctylbithiophen-2-yl)thiophen-2-yl)benzo[1,2-*d*;5,4-*d*′]bisoxazole)] (POBTtBBO) (P2). Polymer obtained as a deep red solid (0.30 g, 65% yield). GPC: M_n = 8200, M_w = 11 400, PDI = 1.39.

Poly(2,6-bis(4-octyl-5-(3,3′-dioctylbithiophen-2-yl)thiophen-2-yl)benzo[1,2-*d*;5,4-*d*′]bisthiazole)] (P3). Polymer obtained as a deep red solid (0.27 g, 55% yield). GPC: M_n = 5000, M_w = 8500, PDI = 1.69.

Device Fabrication and Characterization. *Photovoltaic Cells.* ITO-coated glass substrates were cleaned sequentially by ultrasonication in acetone, methanol, and isopropanol, followed by O_2 plasma exposure for 5 min. PEDOT:PSS aqueous solution was passed through a 0.45 μm PTFE filter, then spin-coated on the ITO substrate at 4000 rpm for 60 s, and dried in a vacuum oven at 120 °C for 1 h. The thickness of PEDOT:PSS layer was ∼40 nm.

All devices were fabricated in a glovebox filled with argon. 50 mg/mL $PC_{71}BM$ in *o*-DCB was prepared by ultrasonic mixing for 1 h and filtered with a 0.45 μm PTFE filter prior to use. The polymers **P1**, **P2**, and **P3** were dissolved in *o*-DCB at 90 °C to yield 10 mg/mL polymer/*o*-DCB solution. The hot solution was quickly filtered with a 0.45 μm PTFE filter before cooling down to room temperature. Subsequently, the polymer and $PC_{71}BM$ in *o*-DCB solutions at different weight ratios of polymer to $PC_{71}BM$ (i.e., 1:0.5, 1:1, 1:2, 1:3, and 1:4) were thoroughly mixed and spin-coated on the PEDOT:PSS surface at 1100 rpm for 40 s. A cathode was prepared by sequentially depositing a Ca film (50 nm) and a Al film (100 nm) through a shadow mask. The photovoltaic devices had an area of 0.10 ± 0.01 cm^2 and were tested under simulated AM 1.5 G irradiation (100 mW cm^{-2}, calibrated with Daystar Meter) using a SoLux solar simulator, and the current−voltage (*I*−*V*) curves were measured using a Keithley 2400 multisource meter.

Atomic Force Microscopy. All measurement were performed on film cast as described above; electrodes were not attached to these samples. A Veeco Digital Instruments atomic force microscope was used to perform the analysis.

Field Effect Transistors. Organic field-effect transistors were fabricated in the bottom gate, bottom contact configuration on heavily doped n-type Si substrates as the gate, and a thermally grown 250 nm silicon dioxide as the dielectric layer (Silicon Quest, dry oxide). The source and drain electrodes were patterned using standard photolithography and were deposited on SiO_2 by sputter deposition of ∼5 nm of titanium and 50 nm of gold. Prior to use, the devices were cleaned for 20 min by exposure to UV light in air (Novascan PSD-UVT) and heat (hot plate, 60−120 °C). The devices were surface treated with OTS in a glovebox for 2 h by immersion in a ∼30 mM solution of OTS in anhydrous trichloroethylene. The devices were then cleaned by rinsing with HPLC grade toluene and dried under nitrogen flow followed by vacuum overnight. **P2** films were spin-casted from a 5 mg/mL solution at 1500 rpm under N_2 and then annealed at 130 °C in glovebox. **P1** and **P3** films were deposited in air by drop-casting 5 μL of a 1 mg mL^{-1} solution in $CHCl_3$ and allowed to dry in a glass Petri dish saturated with $CHCl_3$. After film formation, the devices were further dried overnight in a desiccator under vacuum. FET mobility measurements were performed under a flow of Ar using an Agilent 4155C semiconductor parameter analyzer and a Micromanipulator S6 probe station. When measuring current−voltage curves and transfer curves, V_G was scanned from −80 to +40 V. The field-effect mobilities were obtained from the transfer curves in the saturation regime at V_{DS} = −80 V. A line drawn through the linear part of an $I_{DS}^{1/2}$ vs V_G plot allowed extraction of threshold voltage and field-effect mobilities using the square-law equation for the saturation regime. The average mobilities were obtained from 3 or 4 transistors per polymer film with channel lengths (L) of 10−150 μm.

ASSOCIATED CONTENT

Supporting Information. Synthetic methods for intermediates **4a**, **4b**, **5a**, and **5b**; ^{1}H NMR spectra, X-ray data, fluorescence, DSC traces, and TGA thermographs of **P1**, **P2**, and **P3**. This material is available free of charge via the Internet at http://pubs.acs.org.

AUTHOR INFORMATION

Corresponding Author
*E-mail: malikaj@iastate.edu.

ACKNOWLEDGMENT

We thank the 3M Foundation and the National Science Foundation (DMR-0846607) for financial support.

REFERENCES

(1) Tang, C. W.; VanSlyke, S. A. *Appl. Phys. Lett.* **1987**, *51*, 913.
(2) Burroughes, J. H.; Bradley, D. D. C.; Brown, A. R.; Marks, R. N.; Mackay, K.; Friend, R. H.; Burns, P. L.; Holmes, A. B. *Nature* **1990**, *347*, 539.
(3) Grimsdale, A. C.; Leok Chan, K.; Martin, R. E.; Jokisz, P. G.; Holmes, A. B. *Chem. Rev.* **2009**, *109*, 897.
(4) Tang, C. W. *Appl. Phys. Lett.* **1986**, *48*, 183.
(5) Scharber, M.; Mühlbacher, D.; Koppe, M.; Denk, P.; Waldauf, C.; Heeger, A.; Brabec, C. *Adv. Mater.* **2006**, *18*, 789.
(6) Thompson, B. C.; Frechet, J. M. J. *Angew. Chem., Int. Ed.* **2008**, *47*, 58.
(7) Facchetti, A. *Chem. Mater.* **2010**, *23*, 733.
(8) Brabec, C. J.; Cravino, A.; Meissne, D.; Sariciftci, N. S.; Fromherz, T.; Rispens, M. T.; Sanchez, L.; Hummelen, J. C. *Adv. Funct. Mater.* **2001**, *11*, 374.
(9) Brabec, C. J.; Gowrisanker, S.; Halls, J. J. M.; Laird, D.; Jia, S.; Williams, S. P. *Adv. Mater.* **2010**, *22*, 3839.
(10) Yu, G.; Gao, J.; Hummelen, J. C.; Wudl, F.; Heeger, A. J. *Science* **1995**, *270*, 1789.
(11) Gunes, S.; Neugebauer, H.; Sariciftci Niyazi, S. *Chem. Rev.* **2007**, *107*, 1324.

(12) Coakley, K. M.; McGehee, M. D. *Chem. Mater.* **2004**, *16*, 4533.
(13) van Mullekom, H. A. M.; Vekemans, J. A. J. M.; Havinga, E. E.; Meijer, E. W. *Mater. Sci. Eng., R* **2001**, *32*, 1.
(14) Boudreault, P.-L. T.; Najari, A.; Leclerc, M. *Chem. Mater.* **2010**, *23*, 456.
(15) Zou, Y.; Najari, A.; Berrouard, P.; Beaupre, S.; Reda Aiàch, B.; Tao, Y.; Leclerc, M. *J. Am. Chem. Soc.* **2010**, *132*, 5330.
(16) Liang, Y.; Xu, Z.; Xia, J.; Tsai, S.-T.; Wu, Y.; Li, G.; Ray, C.; Yu, L. *Adv. Mater.* **2010**, *22*, E135.
(17) Chu, T.-Y.; Lu, J.; Beauprea, S.; Zhang, Y.; Pouliot, J.-R.; Wakim, S.; Zhou, J.; Leclerc, M.; Li, Z.; Ding, J.; Tao, Y. *J. Am. Chem. Soc.* **2011**, *133*, 4250.
(18) Liang, Y.; Feng, D.; Wu, Y.; Tsai, S.-T.; Li, G.; Ray, C.; Yu, L. *J. Am. Chem. Soc.* **2009**, *131*, 7792.
(19) Piliego, C.; Holcombe, T. W.; Douglas, J. D.; Woo, C. H.; Beaujuge, P. M.; Frechet, J. M. J. *J. Am. Chem. Soc.* **2010**, *132*, 7595.
(20) Price, S. C.; Stuart, A. C.; Yang, L.; Zhou, H.; You, W. *J. Am. Chem. Soc.* **2011**, *133*, 4625.
(21) Tsao, H. N.; Cho, D. M.; Park, I.; Hansen, M. R.; Mavrinskiy, A.; Yoon, D. Y.; Graf, R.; Pisula, W.; Spiess, H. W.; MuÃàllen, K. *J. Am. Chem. Soc.* **2011**, *133*, 2605.
(22) Wolfe, J. F. Polybenzothiazoles and Polybenzoxazoles. In *Encyclopedia of Polymer Science and Engineering*; John Wiley and Sons: New York, 1988; Vol. 11, p 601.
(23) Wolfe, J. F.; Arnold, F. E. *Macromolecules* **1981**, *14*, 909.
(24) Wolfe, J. F.; Loo, B. H.; Arnold, F. E. *Macromolecules* **1981**, *14*, 915.
(25) Choe, E. W.; Kim, S. N. *Macromolecules* **1981**, *14*, 920.
(26) Inbasekaran, M.; Strom, R. *OPPI Briefs* **1994**, *23*, 447.
(27) Schmitt, R. J.; Ross, D. S.; Hardee, J. R.; Wolfe, J. F. *J. Org. Chem.* **1988**, *53*, 5568.
(28) Alam, M. M.; Jenekhe, S. A. *Chem. Mater.* **2002**, *14*, 4775.
(29) Intemann, J. J.; Mike, J. F.; Cai, M.; Bose, S.; Xiao, T.; Mauldin, T. C.; Roggers, R. A.; Shinar, J.; Shinar, R.; Jeffries-EL, M. *Macromolecules* **2011**, *44*, 248.
(30) Huang, W.; Yin, J. *Polym. Bull.* **2006**, *57*, 269.
(31) Jenekhe, S. A.; Osaheni, J. A. *Chem. Mater.* **1994**, *6*, 1906.
(32) Osaheni, J. A.; Jenekhe, S. A. *J. Am. Chem. Soc.* **1995**, *117*, 7389.
(33) Osaheni, J. A.; Jenekhe, S. A. *Macromolecules* **1993**, *26*, 4726.
(34) Jenekhe, S. A.; Osaheni, J. A.; Meth, J. S.; Vanherzeele, H. *Chem. Mater.* **1992**, *4*, 683.
(35) Reinhardt, B. A.; Unroe, M. R.; Evers, R. C. *Chem. Mater.* **1991**, *3*, 864.
(36) Osaheni, J. A.; Jenekhe, S. A. *Chem. Mater.* **1992**, *4*, 1282.
(37) Babel, A.; Jenekhe, S. A. *J. Phys. Chem. B* **2002**, *106*, 6129.
(38) Guo, P.; Wang, S.; Wu, P.; Han, Z. *Polymer* **2004**, *45*, 1885.
(39) Kricheldorf, H. R.; Domschke, A. *Polymer* **1994**, *35*, 198.
(40) Liu, X.; Xu, X.; Zhuang, Q.; Han, Z. *Polym. Bull.* **2008**, *60*, 765.
(41) Wang, S.; Lei, H.; Guo, P.; Wu, P.; Han, Z. *Eur. Polym. J.* **2004**, *40*, 1163.
(42) Roberts, M. F.; Jenekhe, S. A. *Chem. Mater.* **1993**, *5*, 1744.
(43) Mike, J. F.; Makowski, A. J.; Mauldin, T. C.; Jeffries-EL, M. *J. Polym. Sci., Part A* **2010**, *48*, 1456.
(44) Mike, J. F.; Nalwa, K.; Makowski, A. J.; Putnam, D.; Tomlinson, A. L.; Chaudhary, S.; Jeffries-EL, M. *Phys. Chem. Chem. Phys.* **2011**, *13*, 1338.
(45) Mike, J. F.; Inteman, J. J.; Ellern, A.; Jeffries-EL, M. *J. Org. Chem.* **2010**, *75*, 495.
(46) Mike, J. F.; Makowski, A. J.; Jeffries-EL, M. *Org. Lett.* **2008**, *10*, 4915.
(47) Ahmed, E.; Kim, F. S.; Xin, H.; Jenekhe, S. A. *Macromolecules* **2009**, *42*, 8615.
(48) Osaka, I.; Takimiya, K.; McCullough, R. D. *Adv. Mater.* **2010**, *22*, 4993.
(49) Belfield, K. D.; Yao, S.; Morales, A. R.; Hales, J. M.; Hagan, D. J.; Van Stryland, E. W.; Chapela, V. M.; Percino, J. *Polym. Adv. Technol.* **2005**, *16*, 150.
(50) Ahmed, E.; Subramaniyan, S.; Kim, F. S.; Xin, H.; Jenekhe, S. A. *Macromolecules* **2011**, *44*, 7207.
(51) McEntee, G. J.; Vilela, F.; Skabara, P. J.; Anthopoulos, T. D.; Labram, J. G.; Tierney, S.; Harrington, R. W.; Clegg, W. *J. Mater. Chem.* **2011**, *21*, 2091.
(52) Mamada, M.; Nishida, J.-i.; Tokito, S.; Yamashita, Y. *Chem. Lett.* **2008**, *37*, 766.
(53) Pang, H.; Vilela, F.; Skabara, P. J.; McDouall, J. J. W.; Crouch, D. J.; Anthopoulos, T. D.; Bradley, D. D. C.; de Leeuw, D. M.; Horton, P. N.; Hursthouse, M. B. *Adv. Mater.* **2007**, *19*, 4438.
(54) Wolfe, J. F. *Proc. SPIE* **1987**, *682*, 70.
(55) Tsai, H.-H. G.; Chou, L.-C.; Lin, S.-C.; Sheu, H.-S.; Lai, C. K. *Tetrahedron Lett.* **2009**, *50*, 1906.
(56) Mike, J. F.; Intemann, J. J.; Cai, M.; Xiao, T.; Shinar, R.; Shinar, J.; Jeffries-EL, M. *Polym. Chem.* **2011**, *2*, 2299.
(57) Kokubo, H.; Sato, T.; Yamamoto, T. *Macromolecules* **2006**, *39*, 3959.
(58) McCullough, R. D.; Lowe, R. D.; Jayaraman, M.; Anderson, D. L. *J. Org. Chem.* **1993**, *58*, 904.
(59) McCullough, R. D.; Tristam-Nagle, S.; Williams, S. P.; Lowe, R. D.; Jayaraman, M. *J. Am. Chem. Soc.* **1993**, *115*, 4910.
(60) Liu, J.; Zhang, R.; Sauve, G.; Kowalewski, T.; McCullough, R. D. *J. Am. Chem. Soc.* **2008**, *130*, 13167.
(61) Guo, X.; Kim, F. S.; Jenekhe, S. A.; Watson, M. D. *J. Am. Chem. Soc.* **2009**, *131*, 7206.
(62) Ko, S.; Mondal, R.; Risko, C.; Lee, J. K.; Hong, S.; McGehee, M. D.; Bredas, J.-L.; Bao, Z. *Macromolecules* **2010**, *43*, 6685.
(63) Mei, J.; Heston, N. C.; Vasilyeva, S. V.; Reynolds, J. R. *Macromolecules* **2009**, *42*, 1482.
(64) Beaujuge, P. M.; Amb, C. M.; Reynolds, J. R. *Acc. Chem. Res.* **2010**, *43*, 1396.
(65) Miyamae, T.; Yoshimura, D.; Ishii, H.; Ouchi, Y.; Miyazaki, T.; Koike, T.; Yamamoto, T.; Muramatsu, Y.; Etori, H.; Maruyama, T.; Seki, K. *Synth. Met.* **1997**, *84*, 939.
(66) Koster, L. J. A.; Mihailetchi, V. D.; Blom, P. W. M. *Appl. Phys. Lett.* **2006**, *88*, 093511.
(67) Cardona, C. M.; Li, W.; Kaifer, A. E.; Stockdale, D.; Bazan, G. C. *Adv. Mater.* **2011**, *23*, 2367.
(68) Li, Y.; Wu, Y.; Ong, B. S. *Macromolecules* **2006**, *39*, 6521.
(69) Zhang, R.; Li, B.; Iovu, M. C.; Jeffries-EL, M.; Sauve, G.; Cooper, J.; Jia, S.; Tristram-Nagle, S.; Smilgies, D. M.; Lambeth, D. N.; McCullough, R. D.; Kowalewski, T. *J. Am. Chem. Soc.* **2006**, *128*, 3480.
(70) Li, G.; Shrotriya, V.; Huang, J. S.; Yao, Y.; Moriarty, T.; Emery, K.; Yang, Y. *Nature Mater.* **2005**, *4*, 864.
(71) Park, S. H.; Roy, A.; Beaupre, S.; Cho, S.; Coates, N.; Moon, J. S.; Moses, D.; Leclerc, M.; Lee, K.; Heeger, A. J. *Nature Photonics* **2009**, *3*, 297.
(72) Boudreault, P. L. T.; Najari, A.; Leclerc, M. *Chem. Mater.* **2011**, *23*, 456.